

Supplementary information

Formation of the 15 Å phase as the most expanded hydrated mineral in cold subduction zone

Yoonah Bang^{1,2}, Juhyeok Kim³, Jinhyuk Choi¹, Heehyeon Sim¹, Dongzhou Zhang^{4,5}, Tae-Yeol Jeon⁶, Tae Joo Shin⁷, Hanns-Peter Liermann⁸, Kideok D. Kwon³, and Yongjae Lee^{1,*}

¹Department of Earth System Sciences, Yonsei University, Seoul 03722, Republic of Korea

²Korea Atomic Energy Research Institute (KAERI), Daejeon 34057, Republic of Korea

³Department of Geology, Kangwon National University, Chuncheon 24341, Republic of Korea

⁴Hawaii Institute of Geophysics and Planetology, University of Hawaii at Manoa, Honolulu, HI 96822, USA

⁵GSECARS, University of Chicago, IL 60439, USA

⁶Pohang Accelerator Laboratory, POSTECH, Pohang 37673, Republic of Korea

⁷Graduate School of Semiconductor Materials and Devices Engineering, Ulsan National Institute of Science and Technology (UNIST), Ulsan 44919, Republic of Korea

⁸Photon Sciences, Deutsches Elektronen-Synchrotron (DESY), Hamburg 22607, Germany

*Corresponding author. Email: yongjaelee@yonsei.ac.kr

Table S1. Experimental P-T conditions of Talc with NaHCO₃ (*aq*), NaCl (*aq*), and H₂O (*l*) medium along cold subduction geotherm.

Talc + NaHCO ₃ (<i>aq</i>)	Talc + NaCl (<i>aq</i>)	Talc + H ₂ O (<i>l</i>)
2.6(1) GPa, 70±5 °C	2.4(1) GPa, 65±5 °C	2.3(1) GPa, 205±10 °C
2.6(1) GPa, 150±10 °C	2.4(1) GPa, 90±5 °C	2.3(1) GPa, 225±10 °C
2.4(1) GPa, 175±10 °C	2.7(1) GPa, 110±10 °C	3.2(2) GPa, 310±20 °C
2.5(1) GPa, 175±10 °C	2.9(1) GPa, 135±10 °C	3.8(2) GPa, 335±20 °C
2.6(1) GPa, 175±10 °C	3.1(1) GPa, 180±10 °C	4.0(2) GPa, 365±20 °C
2.5(1) GPa, 200±10 °C	3.0(1) GPa, 200±10 °C	4.3(2) GPa, 370±20 °C
2.6(1) GPa, 210±10 °C	2.7(1) GPa, 240±10 °C	4.4(2) GPa, 400±25 °C
2.6(1) GPa, 215±10 °C	2.9(1) GPa, 245±10 °C	4.5(3) GPa, 420±30 °C
2.7(1) GPa, 275±10 °C	2.9(1) GPa, 265±10 °C	4.7(3) GPa, 425±30 °C
2.6(1) GPa, 280±10 °C	3.0(1) GPa, 290±10 °C	4.7(3) GPa, 445±30 °C
2.8(1) GPa, 280±10 °C	3.0(2) GPa, 325±20 °C	4.8(3) GPa, 475±30 °C
2.9(2) GPa, 295±20 °C	3.2(2) GPa, 330±20 °C	4.3(3) GPa, 505±30 °C
2.7(2) GPa, 335±20 °C	3.3(2) GPa, 330±20 °C	4.4(3) GPa, 550±30 °C
2.8(2) GPa, 340±20 °C	4.0(2) GPa, 330±20 °C	4.5(3) GPa, 570±30 °C
2.8(2) GPa, 345±20 °C	4.0(2) GPa, 355±20 °C	
2.9(2) GPa, 345±20 °C	4.4(2) GPa, 360±20 °C	
3.0(2) GPa, 350±20 °C	4.8(2) GPa, 385±20 °C	
3.5(2) GPa, 365±20 °C	5.0(2) GPa, 400±25 °C	
3.7(2) GPa, 400±20 °C	5.1(3) GPa, 415±30 °C	
4.2(2) GPa, 420±20 °C	5.7(3) GPa, 455±30 °C	
4.4(2) GPa, 470±20 °C	5.9(3) GPa, 470±30 °C	
5.3(3) GPa, 480±30 °C	6.3(3) GPa, 500±30 °C	
5.8(4) GPa, 515±30 °C	6.6(3) GPa, 505±30 °C	
	6.8(3) GPa, 520±30 °C	
	7.2(3) GPa, 540±30 °C	
	7.7(3) GPa, 560±30 °C	

Table S2. Pressure and temperature (P-T) dependent evolution of basal d_{001} spacing of talc and its hydration products, i.e., ‘super-hydrated’ 15 Å phase and 10 Å phase with NaHCO₃ (aq), NaCl (aq), and H₂O (l) medium (see Fig. S2).

NaHCO ₃ + H ₂ O			NaCl + H ₂ O			H ₂ O		
P-T	talc	15 Å phase	P-T	talc	10 Å phase	P-T	talc	10 Å phase
2.6(1) GPa, 70±5 °C	9.057(2)		2.4(1) GPa, 65±5 °C	9.036(1)		3.2(2) GPa, 310±20 °C	9.090(1)	
2.6(1) GPa, 175±10 °C	9.052(1)		2.7(1) GPa, 240±10 °C	9.038(1)		3.8(2) GPa, 335±20 °C	9.041(1)	
2.5(1) GPa, 200±10 °C	9.051(1)		3.0(1) GPa, 290±10 °C	9.019(1)		4.0(2) GPa, 365±20 °C	9.034(1)	
2.6(1) GPa, 215±10 °C	9.046(2)		3.2(2) GPa, 330±20 °C	9.007(1)		4.3(2) GPa, 370±20 °C	9.006(1)	
2.7(1) GPa, 275±10 °C	9.053(1)		4.0(2) GPa, 330±20 °C	8.951(1)		4.4(2) GPa, 400±25 °C	9.010(1)	
2.8(1) GPa, 280±10 °C	9.045(2)		4.0(2) GPa, 355±20 °C	8.937(1)		4.5(3) GPa, 420±30 °C	9.008(1)	9.686(5)
2.9(2) GPa, 295±20 °C	9.046(2)		4.4(2) GPa, 360±20 °C	8.923(1)		4.7(3) GPa, 445±30 °C	8.994(1)	9.631(6)
2.9(2) GPa, 345±20 °C	9.029(1)		4.8(2) GPa, 385±20 °C		9.513(4)	4.8(3) GPa, 475±30 °C	8.998(1)	9.646(3)
3.0(2) GPa, 350±20 °C	9.025(5)	14.428(11)	5.0(2) GPa, 400±25 °C		9.518(5)	4.3(3) GPa, 505±30 °C	9.047(1)	9.683(3)
3.5(2) GPa, 365±20 °C	8.997(2)	14.344(3)	5.7(3) GPa, 455±30 °C		9.459(2)	4.4(3) GPa, 550±30 °C	9.046(1)	9.652(5)
3.7(2) GPa, 400±20 °C	9.011(3)	14.353(5)	5.9(3) GPa, 470±30 °C		9.427(1)	4.5(3) GPa, 570±30 °C	9.052(2)	9.699(6)
4.2(2) GPa, 420±20 °C	8.971(2)	14.237(7)	6.3(3) GPa, 500±30 °C		9.398(1)			
4.4(2) GPa, 470±20 °C	8.945(3)	14.172(6)	6.8(3) GPa, 530±30 °C					
5.3(3) GPa, 480±30 °C	8.913(3)	10.401(8)*	7.7(3) GPa, 560±30 °C					
5.8(4) GPa, 515±30 °C	9.057(2)	9.760(20)*	release					
release		10.299(1)*						

Table S3. Pressure dependent evolution of d_{001} -spacing of talc and ‘super-hydrated’ 15 Å phase up to 7.0(1) GPa after heating at 2.5(1) GPa and 250 °C*.

Pressure (GPa)	talc ($d_{001} = 9.4$ Å)	15 Å phase ($d_{001} = 15.2$ Å)
0	9.370(2)	
0.5(1)	9.261(1)	
1.0(1)	9.173(1)	
1.5(1)	9.114(1)	
2.2(1)	9.049(1)	
2.5(1)	9.012(1)	
3.8(1)*	8.883(1)	13.911(3)
4.4(1)	8.847(1)	13.831(4)
5.6(1)	8.813(1)	13.733(4)
6.0(1)	8.811(1)	13.709(7)
6.5(1)	8.784(1)	13.647(4)
7.0(1)	8.777(2)	13.638(5)
6.0(1)	8.797(1)	13.659(7)
5.0(1)	8.833(1)	13.765(8)
4.1(1)	8.897(1)	13.901(4)
2.1(1)	9.065(1)	14.316(3)
1.3(1)	9.169(1)	14.745(3)
0.5(1)	9.267(1)	15.079(9)
0	9.362(1)	15.216(9)

Table S4. Calculated linear compressibility (along the c -axis and d_{001} -spacing) of talc and its products using Murnaghan equation of state up to 7 GPa. The results from previous study at ambient temperature are shown for comparison¹. The parameters are derived by least-squares regression, using EOSFit, of the observed data to the Murnaghan equation of state: $P_{VT} = K_{0T}/K'_{0T}[(V_{0T}/V)^{(K'_{0T})}-1]$ ($K'=14$).

phase	β_c (x 10 ⁻² GPa ⁻¹)	$\beta_{d_{001}}$ (x 10 ⁻² GPa ⁻¹)	references
talc	1.42	1.34	Gleason et al., 2008
	–	1.51	this study
15 Å	–	4.16	this study
10 Å	2.13	2.03	Comodi et al., 2006

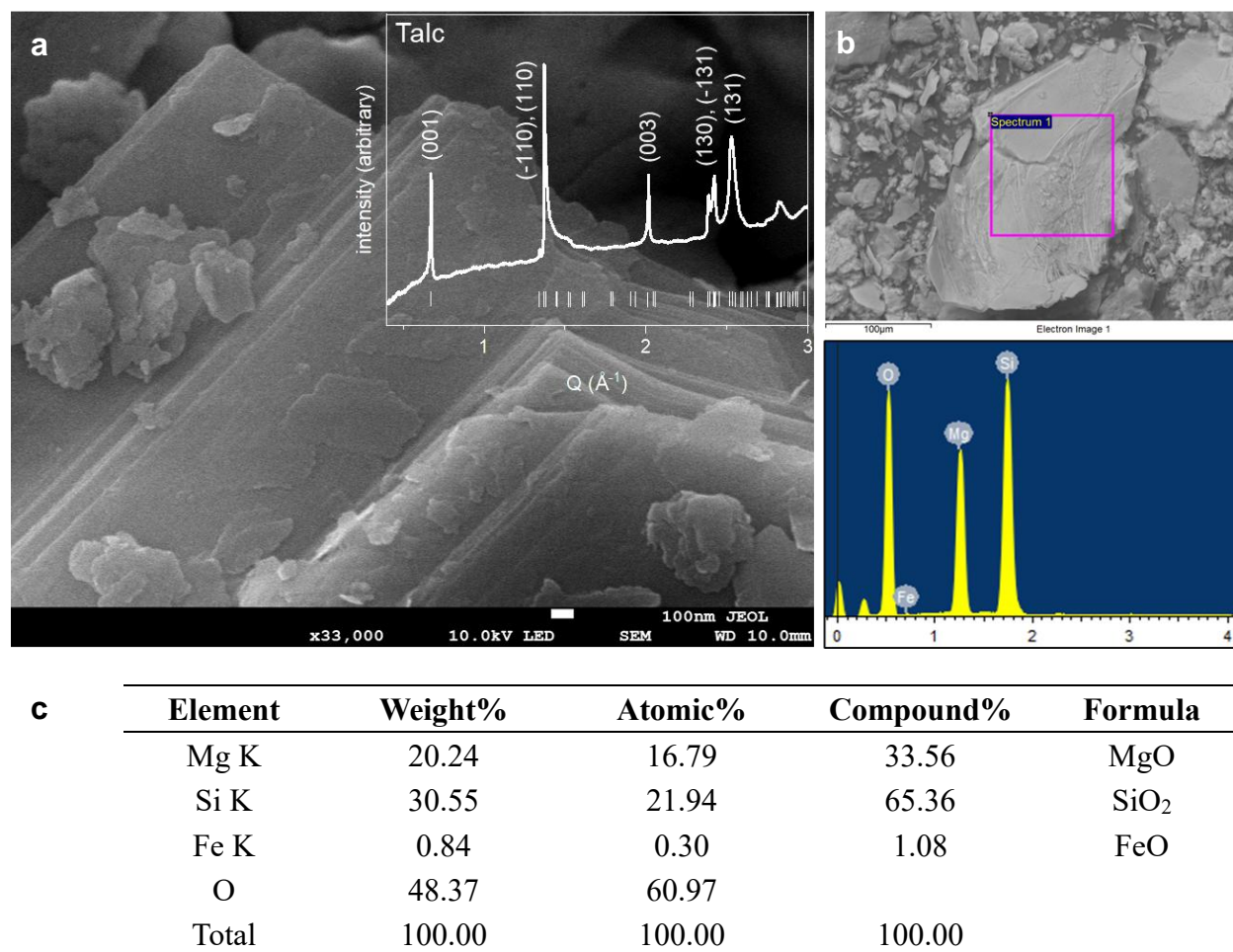


Fig. S1. X-ray diffraction (XRD) and Scanning electron microscopy (SEM) image with Energy dispersive X-ray Spectroscopy (EDS) on natural talc sample. (a) SEM image of natural talc shows layered morphology. The inset shows the XRD pattern of talc powder at ambient condition. The positions of the (hkl) reflections of talc are shown as white vertical bars. Talc has space group $C\bar{1}$ with refined cell parameters of $a = 5.3172(9) \text{ \AA}$, $b = 9.1666(6) \text{ \AA}$, $c = 9.4890(15) \text{ \AA}$, $\alpha = 90.779(11)^\circ$, $\beta = 99.064(14)^\circ$, $\gamma = 89.923(8)^\circ$. (b) EDS analysis of the talc sample (top) and its spectrum (bottom) show elements such as Mg, Si, Fe, and O. (c) Table shows the obtained semi-quantitative elemental analysis results to derive the chemical formula of talc, $(\text{Mg}_{3-x}\text{Fe}_x)\text{Si}_4\text{O}_{10}(\text{OH})_2$ ($x < 0.05$).

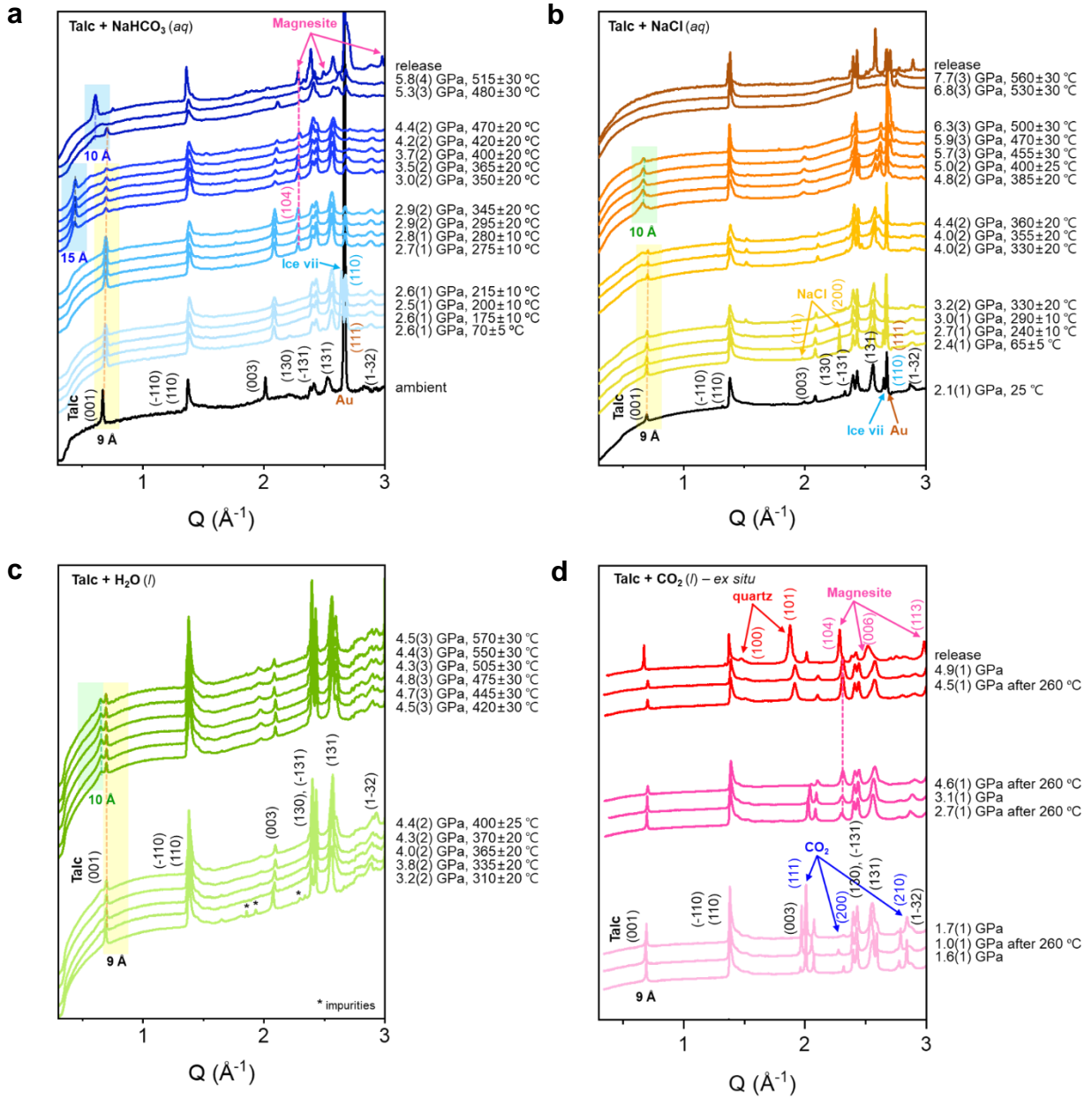


Fig. S2. X-ray powder diffraction patterns of talc with different pressure medium such as (a) NaHCO_3 solution, (b) NaCl solution, (c) H_2O (distilled water), and (d) CO_2 (liquid at HP-HT).

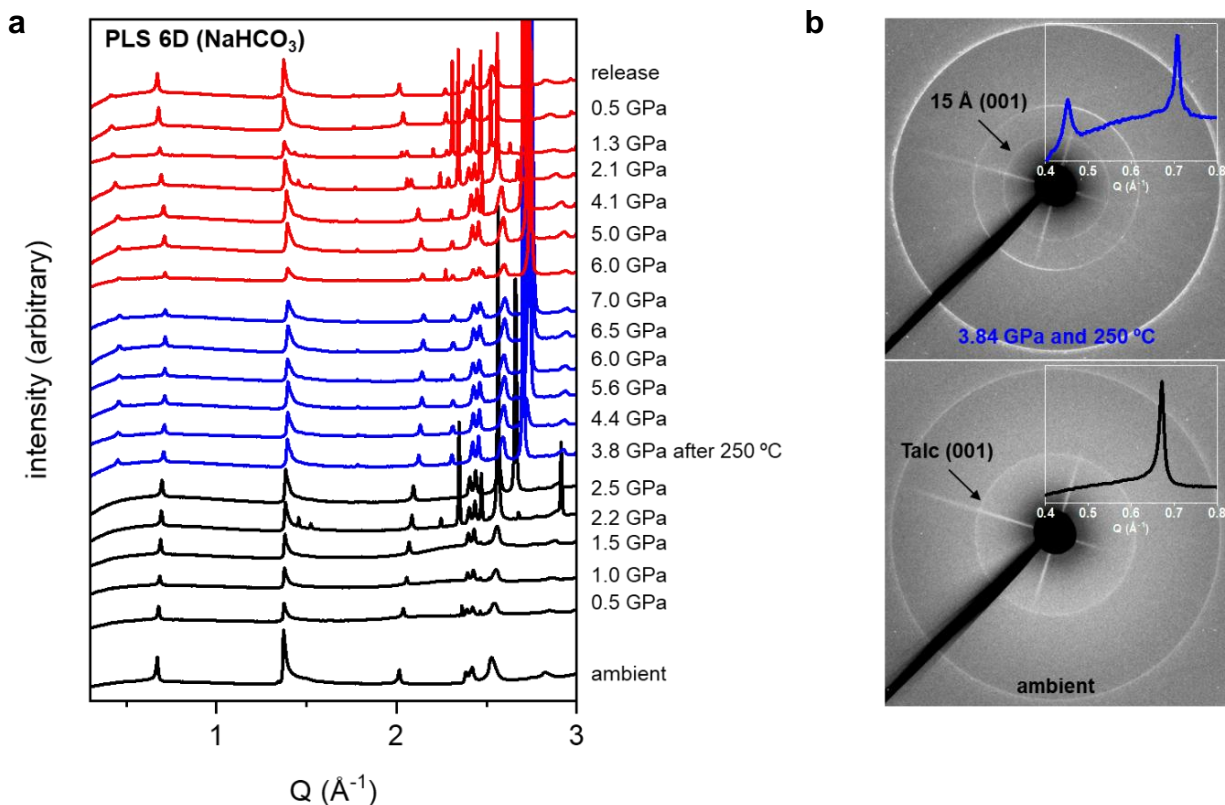


Fig. S3. XRD patterns and selected Debye Scherrer images of talc to emphasize the formation of the super-hydrated 15 Å phase under NaHCO₃ solution medium. (a) XRD patterns of talc and its breakdown products under NaHCO₃ medium at different pressures. The black patterns were measured upon compression before heating, blue patterns upon compression after heating, and red patterns upon decompression. (b) Debye Scherrer images of talc at ambient condition (bottom) and the quenched product after heating at 250 °C and 2.5 GPa (top). Each Inset shows the corresponding XRD pattern to emphasize the formation of the 15 Å *d*-spacing after the pressure and temperature treatment.

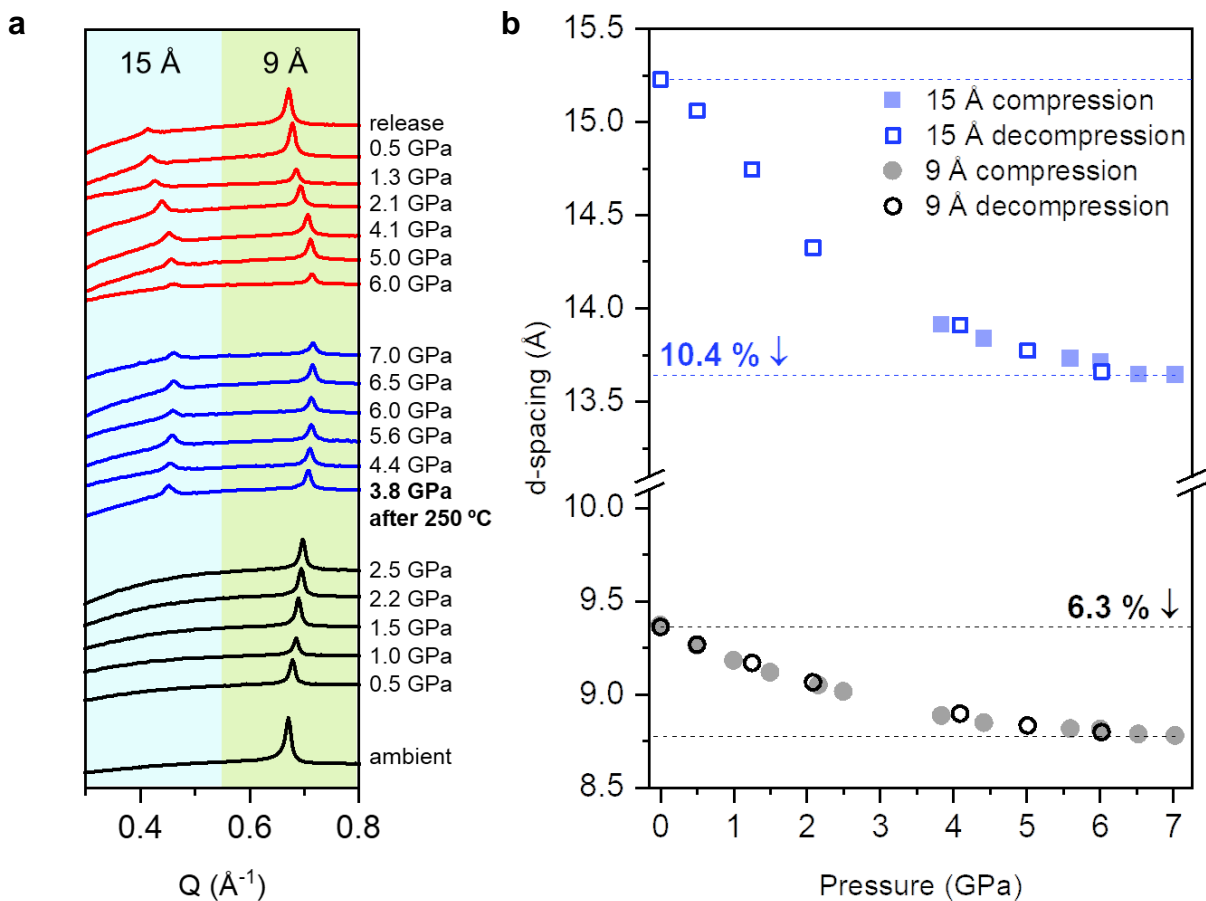


Fig. S4. Pressure dependent evolution of the basal d -spacing of talc and the super-hydrated 15 Å phase. (a) Stacked XRD patterns of talc under NaHCO₃ fluid medium at increasing pressures. Black patterns are upon compression before heating, blue patterns upon compression after heating to show the formation of the super-hydrated 15 Å phase, and red patterns upon decompression. (b) d_{001} -spacing values of talc and the super-hydrated 15 Å as a function of pressure up to ~7.0(1) GPa. Each symbol represents d_{001} spacings of talc (black circle) and the 15 Å phase (blue square) during compression (filled) and decompression (open).

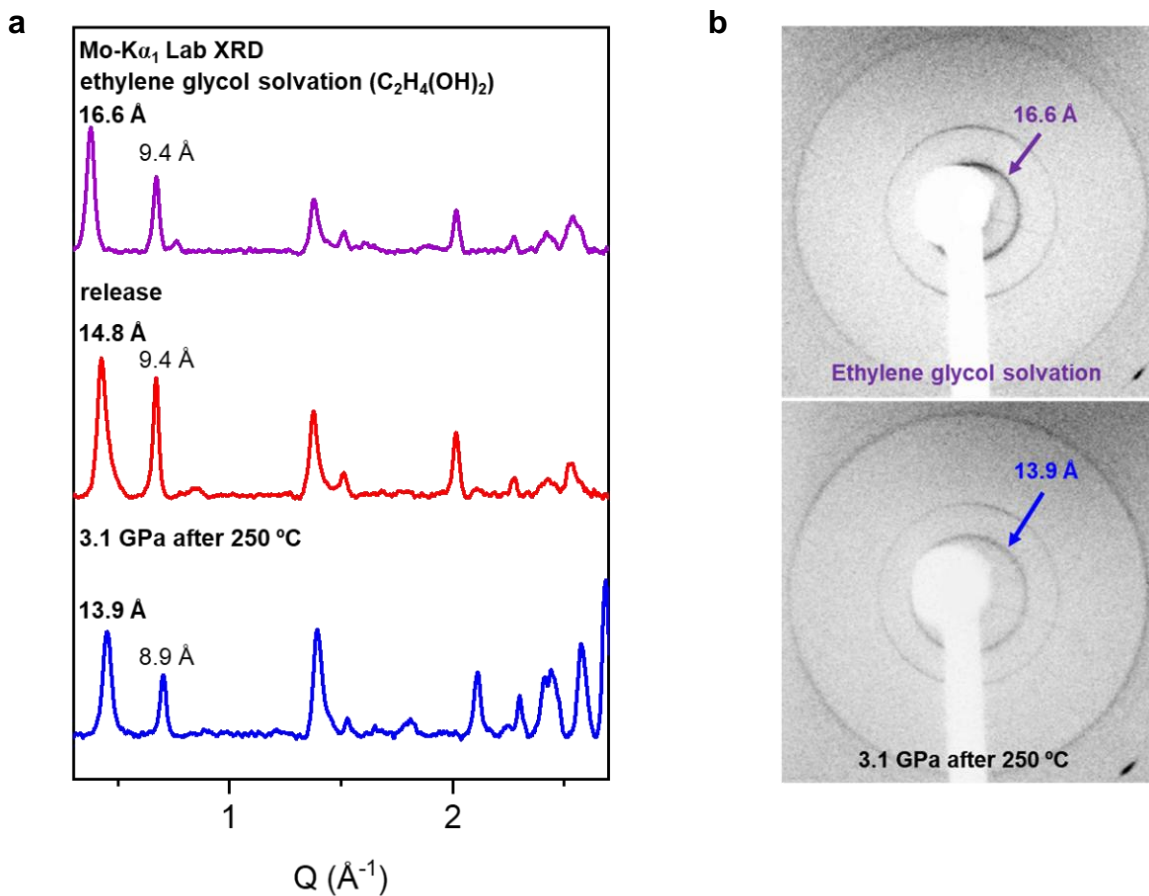


Fig. S5. Ethylene glycol solvation on the recovered 15 Å phase. (a) XRD patterns upon the formation of the 15 Å phase at 3.1 GPa after heating to 250 °C (blue), upon pressure release (red), and after Ethylene glycol solvation (purple). (b) Debye Scherrer images of talc and the 15 Å phase at 3.1 GPa after heating to 250 °C (bottom) and after ethylene glycol treatment (top).

References

- 1 Gleason, A. E., Parry, S. A., Pawley, A. R., Jeanloz, R. & Clark, S. M. Pressure-temperature studies of talc plus water using X-ray diffraction. *Am. Mineral.* **93**, 1043-1050 (2008).